

Standard big bang nucleosynthesis and primordial CNO Abundances after *Planck*

Alain Coc^{a,1}, Jean-Philippe Uzan^{b,c} and Elisabeth Vangioni^{b,c}

^aCentre de Sciences Nucléaires et de Sciences de la Matière (CSNSM), CNRS/IN2P3, Université Paris Sud 11, UMR 8609, Bâtiment 104, F-91405 Orsay Campus (France)

^bInstitut d'Astrophysique de Paris, UMR-7095 du CNRS, Université Pierre et Marie Curie, 98 bis bd Arago, 75014 Paris (France)

^cSorbonne Universités, Institut Lagrange de Paris, 98 bis bd Arago, 75014 Paris (France).

E-mail: coc@csnsm.in2p3.fr, uzan@iap.fr, vangioni@iap.fr

Abstract. Primordial or big bang nucleosynthesis (BBN) is one of the three historical strong evidences for the big bang model. The recent results by the *Planck* satellite mission have slightly changed the estimate of the baryonic density compared to the previous WMAP analysis. This article updates the BBN predictions for the light elements using the cosmological parameters determined by *Planck*, as well as an improvement of the nuclear network and new spectroscopic observations. There is a slight lowering of the primordial Li/H abundance, however, this lithium value still remains typically 3 times larger than its observed spectroscopic abundance in halo stars of the Galaxy. According to the importance of this "lithium problem", we trace the small changes in its BBN calculated abundance following updates of the baryonic density, neutron lifetime and networks. In addition, for the first time, we provide confidence limits for the production of ⁶Li, ⁹Be, ¹¹B and CNO, resulting from our extensive Monte Carlo calculation with our extended network. A specific focus is cast on CNO primordial production. Considering uncertainties on the nuclear rates around the CNO formation, we obtain $\text{CNO}/\text{H} \approx (5 - 30) \times 10^{-15}$. We further improve this estimate by analyzing correlations between yields and reaction rates and identified new influential reaction rates. These uncertain rates, if *simultaneously* varied could lead to a significant increase of CNO production: $\text{CNO}/\text{H} \sim 10^{-13}$. This result is important for the study of population III star formation during the dark ages.

¹Corresponding author.

Contents

1	Introduction	1
2	Primitive observational abundances: update	2
2.1	^4He , D, ^3He and ^7Li observations	2
2.2	^6Li , ^9Be , B, CNO observations	3
3	Effects of $\Omega_b h^2$, τ_n changes and network extension	4
4	Method	6
4.1	Monte Carlo	6
4.2	Reaction rates and uncertainties	9
5	Results concerning ^4He, D, ^3He and ^7Li	10
6	Results concerning ^6Li, ^9Be, B, C	10
A	Appendix: Relation between η and $\Omega_b h^2$	18

1 Introduction

There are three historical observational evidences for the big bang model: the cosmic expansion, the Cosmic Microwave Background (CMB) radiation and primordial or big bang nucleosynthesis (BBN). Today, they are complemented by a large number of evidences in particular from the properties of the large scale structures (see e.g. Peter & Uzan [51] for a textbook description). BBN predicts the primordial abundances of the “light cosmological nuclei”: ^4He , D, ^3He and ^7Li that are produced during the first 20 min after the big bang when the Universe was dense and hot enough for nuclear reactions to take place (see e.g. Fields [28], Iocco et al. [38], Steigman [70] for recent reviews). The comparison of the calculated and observed abundances shows an overall good agreement except for the ^7Li . The essential cosmological parameter of the model is the baryonic density Ω_b . It is related to the baryon to photon ratio, $\eta \equiv n_b/n_\gamma = 2.738 \times 10^{-8} \Omega_b h^2$ (see the appendix) that remains constant during the expansion after the electron–positron annihilation. $\Omega_b h^2$ is now well measured from the angular power spectrum of the CMB temperature anisotropies. A precise value for this, previously free, parameter was provided by the Wilkinson Microwave Anisotropy Probe (WMAP9) satellite, $\Omega_b h^2 = 0.02243 \pm 0.00055$, (“Nine-year (MASTER)”, Hinshaw et al. [33]) while the recent *Planck* mission updated it to $\Omega_b h^2 = 0.02218 \pm 0.00026$ (“*Planck*+lensing+WP+highL”, *Planck* Collaboration XVI [55]). This value is chosen because it includes all the last cosmological constraints. We calculate here the ^4He , D, ^3He and ^7Li primordial abundances by Monte Carlo, using our extended 424 nuclear reaction network [17], also taking into account the updated value of the neutron lifetime [58]. In standard big bang nucleosynthesis, only traces of other isotopes are produced: ^6Li , ^9Be , ^{10}B , ^{11}B and CNO. The CNO abundance is of peculiar interest since it may affect Pop III stellar evolution in the first structures of the Universe. The value which could impact this evolution is estimated to be 10^{-11} [11] or even as low as 10^{-13} (in number of atoms relative to hydrogen,

CNO/H) for the less massive stars [27]. In this context, it is important to evaluate carefully the BBN CNO abundance. In our previous work [17] we obtained a much lower value $\text{CNO}/\text{H}=0.7 \times 10^{-15}$ but no upper nor lower limit (see also Ref. [37]). In this paper, we use the results of our Monte Carlo calculations *i*) to estimate the uncertainties on the BBN production of the minor isotopes, and in particular of CNO and *ii*) analyze the correlations between reaction rates and isotopic abundances to identify potentially important reactions that were not identified in our previous sensitivity analysis. We show that by calculating correlations, we find important reactions that were overlooked in sensitivity studies changing one reaction at a time. This is crucial because the level of the CNO abundance plays a key role in the evolution of the first stars.

2 Primitive observational abundances: update

2.1 ^4He , D, ^3He and ^7Li observations

Deuterium is a very fragile isotope, easily destroyed after BBN. Its most primitive abundance is determined from the observation of cosmological clouds at high redshift, on the line of sight of distant quasars. Very few such observations are available [52]. Up to now, the observation of about 10 quasar absorption systems gave the weighted mean abundance of deuterium $\text{D}/\text{H} = (3.02 \pm 0.23) \times 10^{-5}$ [49]. However, these individual measurements of D/H show a considerable scatter and it is likely that systematic errors dominate the uncertainties. Recently, Cooke et al. [21, 53] have done new observations of Damped Lyman- α (DLA) systems at high redshift and made a global reanalysis, including previous observations, that lead to a new mean value of

$$\text{D}/\text{H} = (2.53 \pm 0.04) \times 10^{-5}, \quad (2.1)$$

lower and with a much narrower error bar than in previous determinations.

After BBN, ^4He is still produced by stars. Its primitive abundance is deduced from observations in HII (ionized hydrogen) regions of compact blue galaxies. The primordial ^4He mass fraction, Y_p , is obtained from the extrapolation to zero metallicity but is affected by systematic uncertainties [6, 41] such as plasma temperature or stellar absorption. Recently, Aver et al. [7, 8], using a subset of the data set found in Izotov et al ([40, 42], and references therein) have incorporated new atomic data and updated their recent Markov Chain Monte Carlo analysis; so they have determined the primordial helium abundance by a regression to zero metallicity (however within a narrow range of metallicity),

$$Y_p = 0.2465 \pm 0.0097 \quad (2.2)$$

which corresponds to a narrower error bar than previous constraints. This is the value we use to compare with our calculations. Another recent determination of Izotov et al. [42], $Y_p = 0.254 \pm 0.003$ is higher than the Aver et al. [8] value. The difference comes from a different a regression to zero metallicity (the mean value, i.e. with no regression, $Y_p = 0.2535 \pm 0.0036$ of Aver et al. [8] and the Izotov et al. [42] one are in perfect agreement) and differences in the atomic physics involved.

Contrary to ^4He , ^3He is both produced and destroyed in stars throughout its galactic evolution, so that the evolution of its abundance as a function of time is subject to large uncertainties. ^3He has been observed in our Galaxy [9], and one only gets a 'local' constraint

$$^3\text{He}/\text{H} = (1.1 \pm 0.2) \times 10^{-5}. \quad (2.3)$$

This observation is consistent with the BBN predicted value, nevertheless, due to these uncertainties related to stellar evolution, it is difficult to use it as a constraint.

Primitive lithium abundance is deduced from observations of low metallicity stars in the halo of our Galaxy where the lithium abundance is almost independent of metallicity, displaying the so-called Spite plateau [66]. This interpretation assumes that lithium has not been depleted at the surface of these stars, so that the presently observed abundance can be assumed to be equal to the primitive one. The small scatter of values around the Spite plateau is indeed an indication that depletion may not have been very efficient. However, at very low metallicity, on top of a lot of scatter, a slight decrease of Li with metallicity appears. In this context, Spite & Spite [67] pointed out that the abundance of lithium could be even lower when extrapolating toward zero-metal stars, just after the Big Bang. So, considering the Spite plateau, there is a discrepancy between the value *i)* deduced from these observed spectroscopic abundances and *ii)* the BBN theoretical predictions assuming Ω_b is determined by the CMB observations. Many studies have been devoted to the resolution of this so-called *Lithium problem* and many possible “solutions”, none fully satisfactory, have been proposed. For a detailed analysis see Fields [28], the proceedings of the meeting “Lithium in the cosmos” [39] and recently Cyburt et al. [23]. Note that recent lithium observations [34] have been done in the Small Magellanic Cloud which is a nearby irregular galaxy with quarter of the sun’s metallicity and its abundance is found to be nearly equal to the BBN one. It could be a strong constraint for the lithium galactic evolution. Astronomical observations of these metal poor halo stars [60] have thus led to a relative primordial abundance of $\text{Li}/\text{H} = (1.23^{+0.34}_{-0.16}) \times 10^{-10}$ while a more recent analysis [62] gives

$$\text{Li}/\text{H} = (1.58^{+0.35}_{-0.28}) \times 10^{-10} \quad (2.4)$$

which we use in our analysis. For reviews on the Li observations, we refer to Spite & Spite [67] and Frebel & Norris [29].

2.2 ${}^6\text{Li}$, ${}^9\text{Be}$, B, CNO observations

The origin of the light elements LiBeB, is a crossing point between optical and gamma spectroscopy, non thermal nucleosynthesis (via spallation with Galactic Cosmic Rays, GCR), stellar evolution and Big Bang nucleosynthesis. Lithium-6 is also observed in metal poor stars, as discussed above for ${}^7\text{Li}$. Its observational history is peculiar. In the past, Asplund et al. [4] have provided observations of ${}^6\text{Li}/{}^7\text{Li}$ ratio which suggesting the presence of a plateau, at typically ${}^6\text{Li}/\text{H} = 10^{-11}$, leading to a possible pre-galactic origin of this isotope (see Rollinde et al. [59]). In a second time, the observational ${}^6\text{Li}$ plateau has been questioned in Cayrel et al. [12] who have considered in more details the line shape asymmetries. Consequently, there has been a retraction concerning the existence of a ${}^6\text{Li}/\text{H}$ plateau [45]. Presently, only one star, HD84937, presents a ${}^6\text{Li}/{}^7\text{Li}$ ratio of the order of 0.05 (see Steffen et al. [68]) and there is no remaining evidence for a plateau at very low metallicity. We hence use this value as an upper limit: ${}^6\text{Li}/\text{H} \lesssim 10^{-11}$ while the prediction of the BBN calculations are ${}^6\text{Li}/\text{H} = 10^{-14}$.

Beryllium has only one stable isotope ${}^9\text{Be}$. As D and Li, it is a fragile nucleus. It is formed in the vicinity of Type II supernovae (SNII) by non thermal process (spallation) (see Vangioni-Flam et al. [73, 74]). It is also observed in metal poor stars. Boesgaard et al. [10] (and references therein) have performed an update of Be observations in metal poor stars which provides a primitive abundance at very low metallicity of the order of $\text{Be}/\text{H} = 3. \times 10^{-14}$

at $[\text{Fe}/\text{H}] = -3.5$. This observation, that we adopt as upper limit of the primordial abundance, has to be compared to the typical primordial Be abundance, $\text{Be}/\text{H} = 10^{-18}$.

Boron has two stable isotopes: ^{10}B and ^{11}B . It is also synthesized by non thermal processes, GCR or neutrinos (for ^{11}B) (see Vangioni-Flam et al. [72, 73], Vangioni-Flam & Cassé [75]). The most recent observations of boron in low metal stars come from Duncan et al. [26] and Garcia-Lopez et al. [30]. In the galactic halo, the lowest boron abundance at $[\text{Fe}/\text{H}] \lesssim -3$. is $\text{B}/\text{H} \approx 10^{-12}$, to be compared to the typical primordial B abundance $\text{B}/\text{H} = 3. \times 10^{-16}$.

For a general review of these light elements, see the IAU Proceedings Edts Charbonnel et al. [13].

Finally, CNO elements are observed in the lowest metal poor stars (around $[\text{Fe}/\text{H}]=-5$). The observed abundance of CNO is typically $[\text{CNO}/\text{H}]=-4$, relatively to the solar abundance i.e. primitive $\text{CNO}/\text{H} < 10^{-7}$. For a review see Frebel & Norris [29] and references therein.

3 Effects of $\Omega_b h^2$, τ_n changes and network extension

Concerning the update of the CMB, a comparison between the columns of Table 1 shows the effect of a change in $\Omega_b h^2$ from Spergel et al. [64] (column 2) to Komatsu et al. [43] (columns 3 or 4; depending on the choice of the neutron lifetime) and to *Planck* Collaboration XVI [55] (column 5). In that way, we can trace the changes in our previous publications e.g. in Coc & Vangioni [15] where we used three-years WMAP only [64], in Coc et al. [17] (seven-years WMAP [43]) until this work (*Planck*+lensing+WP+highL [55]), together with evolving Particle Data Group evaluation of the neutron lifetime, over the years. For the final calculations, we choose, for $\Omega_b h^2$, the value from the Planck paper that incorporate the Planck temperature data, polarization data from the WMAP satellite in the multipole range $2 < \ell < 23$, information from the lensing potential as determined from the trispectrum computed on Planck’s maps [56] and information coming from ground-based high resolution experiments, such as ACT and SPT. This data set, referred to as “Planck+lensing+WP+highL” can be considered to the most uptodate combination of CMB data, hence leading to the most accurate estimation of the cosmological parameters. These changes mostly affects $^7\text{Li}/\text{H}$ by about 4% and D/H by about 2.7% while the other changes are below a percent. Even though it won’t change the nature of the “lithium problem”, we found important to trace the small changes in its BBN calculated abundance following updates of the baryonic density, neutron lifetime and networks. A BBN evaluation has been done by *Planck* Collaboration XVI [55], using $\Omega_b h^2 = 0.02207 \pm 0.00027$; their prediction regarding the Y_p and D/H abundances are similar to ours (0.24725 ± 0.00032 and $2.656 \pm 0.067 \times 10^{-5}$ respectively at η_{CMB}) but they do not provide any $^7\text{Li}/\text{H}$ value. In Table 1, we show the influence of changes in $\Omega_b h^2$ and τ_n with a minimal network. Table 2, compared to Table 1, show the effect of extending the network. Small differences in D and ^7Li are observed but that could not be traced to well identified origins: as we shall see in § 6, there are combined effects of reaction rates that are different from the effects of individual rates. However, changes in neutron late time abundance and sub-dominant ^7Be destruction mechanism like $^7\text{Be}(n,\alpha)^4\text{He}$ [79] play a role. Finally, in Table 3, we compare our Monte Carlo (§ 4.1) results to observations (§ 2.1).

Note that in order to precisely compare our Y_p values with *Planck* Collaboration XVI [55] and some other works, an additional $\Delta Y_p = 0.0018$ correction should be made. The weak reaction rates [25] that we numerically integrate include zero-temperature Coulomb and radiative corrections [25, 47]. This correction amounts to $\Delta Y_p = 0.00316$, in our cal-

Table 1. Primordial abundances with reduced network. (Bold face displayed values highlight parameter changes.)

	(a)	(b)	This work	This work
Nb. reactions	13	15	15	15
$\Omega_b h^2$	$0.0223^{+0.00075}_{-0.00073}$ (c)	0.02249 (e)	0.02249 (e)	0.02207 (g)
τ_n	885.7 ± 0.8 (d)	885.7 (d)	880.1 (f)	880.1
Y_p^*	0.2476 ± 0.0004	0.2475	0.2464	0.2462
D/H ($\times 10^{-5}$)	2.68 ± 0.15	2.64	2.64	2.72
${}^3\text{He}/\text{H}$ ($\times 10^{-5}$)	1.05 ± 0.04	1.05	1.05	1.06
${}^7\text{Li}/\text{H}$ ($\times 10^{-10}$)	5.14 ± 0.50	5.20	5.18	4.98

*An additional $\Delta Y_p = 0.0018$ correction should be made (see text). (a) Coc & Vangioni [15]; (b) Coc et al. [17], (c) Spergel et al. [64]; (d) Amsler et al. [57]; (e) Komatsu et al. [43]; (f) Beringer et al. [58]; (g) *Planck* Collaboration XVI [55]

Table 2. Primordial abundances with extended network.

Nb. reactions	424	424	424
$\Omega_b h^2$	0.02243 (x)	0.02207 (y)	0.02218 ± 0.00026 (z)
τ_n	880.1	880.1	880.1 ± 1.1
Y_p^*	0.2465	0.2463	0.2461–0.2466
D/H ($\times 10^{-5}$)	2.60	2.67	2.57–2.72
${}^3\text{He}/\text{H}$ ($\times 10^{-5}$)	1.04	1.05	1.02–1.08
${}^7\text{Li}/\text{H}$ ($\times 10^{-10}$)	5.13	4.96	4.56–5.34

*An additional $\Delta Y_p = 0.0018$ correction should be made (see text). Hinshaw et al., WMAP9 [33] (y) *Planck* only [55] (z) *Planck*+lensing+WP+highL [55]

calculations at the relevant $\Omega_b h^2$ (0.0031 in Lopez & Turner [47]). What we have neglected, up to now are the finite-nucleon mass correction ($\Delta Y_p = 0.0012$ [47]), finite-temperature radiative correction ($\Delta Y_p = 0.0003$ [47]), QED plasma ($\Delta Y_p = 0.0001$ [47]) and neutrino decoupling ($\Delta Y_p = 0.0002$ [48]), for a total of $\Delta Y_p = 0.0018$, because they cannot be easily directly re-calculated¹. Hence, our quoted Y_p uncertainties reflect the nuclear uncertainties, mainly τ_n , not the theoretical uncertainties on these corrections, difficult to estimate for us. Nevertheless, these neglected corrections (i.e. the $\Delta Y_p = 0.0018$ not included in the above Tables) remain one order of magnitude below the observational uncertainty: 0.2465 ± 0.0097 .

Since the neutron lifetime and baryonic density values are both subject to debate (Beringer et al. [58], Wietfeldt & Greene [80] for τ_n and *Planck* Collaboration XVI [55] and Spergel et al. [65] for $\Omega_b h^2$), instead of providing new tabulated values, we propose fits for the BBN abundances of ${}^4\text{He}$, D, ${}^3\text{He}$ and ${}^7\text{Li}$ abundances as a function of $\Omega_b h^2$, τ_n and N_{eff} (see definition below) hence of the BBN predictions. This can be used to update any column of Tables 1 and 2 with $\Omega_b h^2$ or τ_n different values than those in the same column or for

¹ We numerically calculate the weak rates, to keep track on the dependence w.r.t. G_F (Fermi constant), m_e (electron mass) and Q_{np} (neutron-pronton mass difference), essential in our investigations concerning variations of constants in BBN [14, 18].

$\Delta N_{\text{eff}} = N_{\text{eff}} - 3 \neq 0$. Our motivation is to provide simple fits that could be directly used to calculate the effect induced by the small changes in and $\Omega_b h^2$ or τ_n until their precise values are settled. Fitted BBN abundances were already provided by e.g Iocco et al. [38], Lopez & Turner [47], Steigman [71] but, they η instead of $\Omega_b h^2$ [47] (see the appendix), lack N_{eff} [38] or τ_n [71]. We checked that, for small variations our results are very close to Iocco et al. [38] for τ_n and $\Omega_b h^2$ dependence².

$$\Delta Y_p = +0.4274 \Delta \Omega_b h^2 + 2.043 \times 10^{-4} \Delta \tau_n + 1.348 \times 10^{-2} \Delta N_{\text{eff}} - 9.805 \times 10^{-4} \Delta N_{\text{eff}}^2 \quad (3.1)$$

$$\Delta \text{D}/\text{H} = -1.878 \times 10^{-3} \Delta \Omega_b h^2 + 1.256 \times 10^{-8} \Delta \tau_n + 3.564 \times 10^{-6} \Delta N_{\text{eff}}, \quad (3.2)$$

$$\Delta {}^3\text{He}/\text{H} = -2.783 \times 10^{-4} \Delta \Omega_b h^2 + 1.761 \times 10^{-9} \Delta \tau_n + 5.064 \times 10^{-7} \Delta N_{\text{eff}}, \quad (3.3)$$

$$\Delta {}^7\text{Li}/\text{H} = +4.767 \times 10^{-8} \Delta \Omega_b h^2 + 2.4541 \times 10^{-13} \Delta \tau_n - 4.686 \times 10^{-11} \Delta N_{\text{eff}}. \quad (3.4)$$

These fits also consider the variations induced by a change in $-1 < \Delta N_{\text{eff}} < +1$ where N_{eff} , the effective number of relativistic degrees of freedom, is defined by:

$$\rho_r = \left[1 + \frac{7}{8} N_{\text{eff}} \left(\frac{T_\nu}{T} \right)^4 + \frac{15}{\pi^2} \frac{\rho_e}{T^4} \right] \rho_\gamma. \quad (3.5)$$

At recombination, $\rho_e \ll \rho_r$ and $(T_\nu/T)^4 = (4/11)^{4/3}$, so that Eq. (3.5) matches the definition used in CMB analyses.

4 Method

4.1 Monte Carlo

Coc & Vangioni [15] used a network reduced to the 12 main reactions (13 with the ${}^3\text{H}(\text{p},\gamma){}^4\text{He}$ that plays a negligible role) for which the rate uncertainties are small compared to all other ones, and sampled the rates within the uncertainty range according to a normal distribution. Here, the extended network includes reaction rates that can be uncertain by a factor of a few orders of magnitude due to the lack of experimental data. Hence, we follow Longland et al. [46] and use a lognormal distribution to cope with these large uncertainty factors together with ensuring that the sampled rates are positive:

$$f(x) = \frac{1}{\sigma\sqrt{2\pi}} \frac{1}{x} e^{-(\ln x - \mu)^2 / (2\sigma^2)} \quad (4.1)$$

(with $x \equiv N_A \langle \sigma v \rangle$ for short). This is equivalent to assumption that $\ln(x)$ is Gaussian distributed with expectation value μ and variance σ^2 . For the lognormal distribution, one has:

$$E[x] = e^{(2\mu + \sigma^2)/2}, \quad \text{and} \quad V[x] = e^{(2\mu + \sigma^2)} \left[e^{\sigma^2} - 1 \right]. \quad (4.2)$$

²After a typo, 0.39→0.039 in Iocco et al. [38], Eq. (63), has been corrected.

As discussed in Longland et al. [46] (see their Fig. 1), for small σ a lognormal distribution and a normal distribution with the same expectation value and variance are close to each other. Hence, since the uncertainty in the 12 main reaction rates are small, using here a lognormal distribution for those reactions makes no difference with Coc & Vangioni [15] results.

To perform the Monte Carlo calculation, we follow the prescription of Sallaska et al. [61]. Namely the reaction rates $x_k \equiv N_A \langle \sigma v \rangle_k$, (with k being the index of the reaction), are assumed to follow a lognormal distribution:

$$x_k(T) = \exp(\mu_k(T) + p_k \sigma_k(T)) \quad (4.3)$$

where p_k is sampled according to a *normal* distribution of mean 0 and variance 1 (Eq. (22) of Sallaska et al. [61]). μ_k and σ_k determine the location of the distribution and its width which are tabulated as a function of T :

$$x_{\text{med}} \equiv \exp(\mu) \quad (4.4)$$

is the median rate and

$$f \equiv \exp(\sigma) \quad (4.5)$$

the uncertainty factor. They are deduced from the evaluation of rate uncertainties. For reactions for which “high” and “low” rates³ are available,

$$\mu \equiv \ln \sqrt{x_{\text{low}} \times x_{\text{high}}} \quad (4.6)$$

and

$$\sigma \equiv \ln \sqrt{x_{\text{high}}/x_{\text{low}}} \quad (4.7)$$

(see Longland et al. [46]). To avoid erratic numerical behavior, we limit the sampling to values lower than one thousand times the median rate, i.e.,

$$x < 10^3 x_{\text{med}}, \quad (4.8)$$

to remain within a range already explored [17].

The Monte Carlo calculation proceeds as follows. For each trial labeled by i , we sample randomly a set of $\{p_{k;i}\}$ different numbers where k that runs from 1 to N (number of reactions) is the index of the reaction. Each one follows independently a Gaussian distribution of mean value 0 and variance 1 and is obtained from a standard random number generator. A BBN calculation is performed with the set of reaction rates $\{x_{k;i}\}$ obtained from Eq. (4.3) that produce the set of isotopic abundances $\{y_{j;i}\}$ obtained in trial i . Here, $j=^4\text{He}$, D , ^3He , ^7Li , ^6Li , ^9Be , ^{11}B and CNO is the index the corresponding abundances after decays of radioactive isotopes (^7Be , ^3H , ^{11}C , ...) or summation of $A \geq 12$ isotopic abundances (CNO). For further analyses, for each trial, not only the final abundances are stored in a database but also all the $\{p_{k;i}\}$ values. This allows for correlation studies discussed below.

To obtain the primordial abundances and their uncertainties, as tabulated below, $\Omega_b h^2$ also is randomly sampled, following a Gaussian distribution according to the CMB deduced

³In the literature one often find tables of reaction rates with labels such as “high”, “low”, “upper”, “lower” or “recommended”. In most recent works e.g. Descouvemont et al. [24], Iliadis et al. [35], they have well defined statistical significance. In many older works, e.g. Angulo et al. [3] they have no precise definition but we still use Eqs. (4.6) and (4.7), for lack of anything better, if this is the only source, to calculate μ and σ , to be used in the Monte Carlo. (See Longland et al. [46].)

data. After 30000 such computations, the calculated distributions of abundances are obtained as displayed in Fig. 1 for ${}^7\text{Li}$. The median primordial abundances and associated 68% confidence intervals are then calculated by taking respectively the 0.5, 0.16 and 0.84 quantiles of the abundance distributions (see Fig. 5 in Longland et al. [46]).

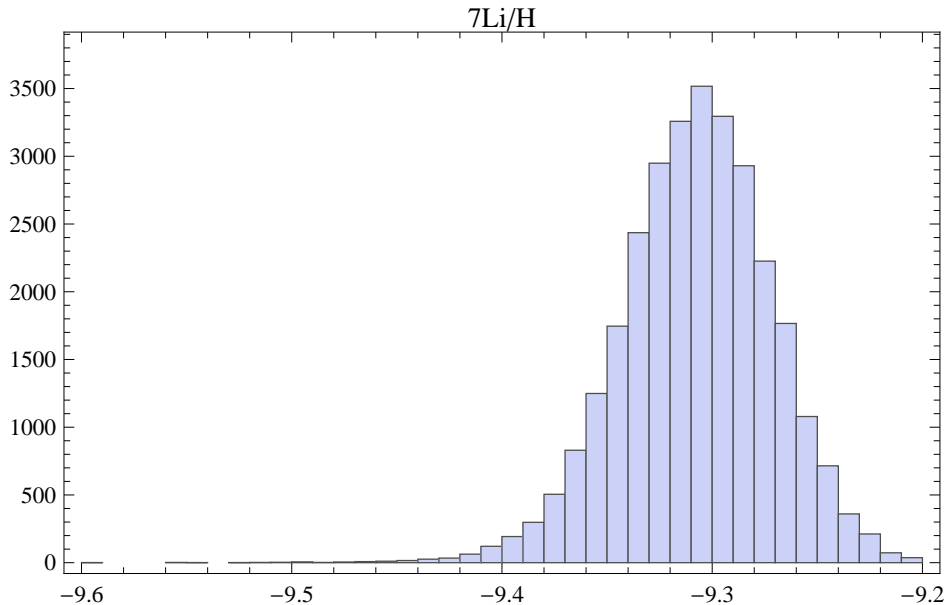


Figure 1. Histogram of the ${}^7\text{Li}/\text{H}$ distribution, from which the median and confidence interval is calculated.

It has been suspected that traditional sensitivity studies, in which only one reaction is varied while the others are held constant, cannot properly address all the important correlations between rate uncertainties and nucleosynthetic predictions [36]. Searching for such correlations was done by Parikh et al. [50] for X-ray bursts (see their Figs. 7 and 8). They have not found new influential reaction, by examining correlations, as compared to their more traditional sensitivity studies. However, we think that it is worth applying this methods to BBN because the density of the “fabric” of a BBN network (d, t and ${}^3\text{He}$ in addition to the usual n, p and α -particles induced reactions) is higher, offering more potential paths. For this purpose, the same Monte Carlo calculation is performed, except that $\Omega_b h^2$ is fixed, to obtain a data base that can be used to study correlations. The Pearson’s correlation coefficient between isotope j and reaction k is, then, calculated as:

$$C_{j,k} = \frac{1}{N} \frac{\sum_{i=1}^N (y_{j;i} p_{k;i} - \overline{y_j} \overline{p_k})}{\sigma_j \sigma'_k} \quad (4.9)$$

where $y_{j;i}$ is again the final abundance of isotope j obtained in trial i with the set of reaction rates $\{x_{k;i}\}$ obtained from Eq. (4.3) with the set of randomly sampled $\{p_{k;i}\}$. The correlation coefficients are calculated, with $y_j \equiv \ln(n_j/n_H)$ for $j \neq {}^4\text{He}$ and $y_{{}^4\text{He}} \equiv Y_p$ for the abundances. In Eq. (4.9), $\overline{y_j}$ [$\overline{p_k}$] and σ_j [σ'_k] stand for the mean and standard deviation of y_j [p_k]. If it were not for the condition (4.8), one would have obviously $\overline{p_k} \equiv 0$ and $\sigma'_k \equiv 1$ since the p_k are sampled according to a normal distribution.

4.2 Reaction rates and uncertainties

In this study, the reaction network and the thermonuclear rates comes from Coc et al. [17]. Namely, it includes 59 nuclides from neutron to ^{23}Na , linked by 391 reactions involving n, p, d, t, ^3He and α -particles induced reactions and 33 β -decay processes [5]. Reaction rates were taken primarily from Angulo et al. [3], Descouvemont et al. [24], Iliadis et al. [35], Xu et al. [81] and other evaluations when available. Following their sensitivity study a few reaction rates were re-evaluated by Coc et al. [17]; they are also used here. The complete list of reactions with associated references to the origin of the rates can be found in Table 4 of Coc et al. [17] (except for $^7\text{Be}(n,\alpha)^4\text{He}$ for which we use here the Wagoner [79] rate instead of the TALYS one in Coc et al. [17]). Since our previous Monte Carlo BBN calculations [15], no change has been made concerning 11 of the 12 main BBN reactions rates. We use those from the evaluation performed by Descouvemont et al. [24] except for $^1\text{H}(n,\gamma)\text{D}$ [2] and $^3\text{He}(\alpha,\gamma)^7\text{Be}$ [22]. A new experiment [44] have provided new data for the $\text{D}(d,n)^3\text{He}$ and $\text{D}(d,n)^3\text{He}$ cross section after the Descouvemont et al. [24] evaluation. Within the BBN energy range, the new data fall exactly on the Descouvemont et al. [24] R-matrix fit (see Fig. 2 of Coc [19]) that has not yet been updated with this new data.

A recent paper by Pizzone et al. [54] provides new evaluation of ^4He , D, ^3He and ^7Li primordial abundances based on new nuclear data, but comparison with this work is difficult. The new data is extracted by an *indirect* experimental method (the Trojan Horse Method) that requires theoretical input. We use instead the results of *direct measurements that provide the same data at, and even below, BBN energies* [24], not affected by screening [77]. Besides, nothing is said of the origin for rate of the $^3\text{He}(\alpha,\gamma)^7\text{Be}$ used in their calculations, which is known to be essential for ^7Li prediction, and has been updated by Cyburt & Davids [22].

The only modification of the main rates concerns the weak reactions involved in $n \leftrightarrow p$ equilibrium whose rates [25] is determined from the standard theory of the weak interaction but needs to be normalized to the experimental neutron lifetime. The latter has recently been revised by the Particle Data Group from 885.7 ± 0.8 s [57], used in Coc & Vangioni [15], to 880.1 ± 1.1 s [58]. This significant change is due to the inclusion of the Serebrov et al. [63] experimental value, now comforted by new analyses (see Beringer et al. [58], Wietfeldt & Greene [80] for more details), that was previously left out of the averaging because of its inconsistency with other data. For this quantity, we use the latest value recommended by the Particle Data Group $\tau_n = 880.1 \pm 1.1$ s [58], but are aware that this remains an open debate [80] but that affects essentially, only ^4He .

The calculation of $^6\text{Li}/\text{H}$ depends directly on the $\text{D}(\alpha,\gamma)^6\text{Li}$ reaction rate that was plagued with by large uncertainty [3], New measurement of the $\text{D}(\alpha,\gamma)^6\text{Li}$ which is the main way to produce primordial ^6Li have been performed. In the absence of direct measurements at BBN energy, Hammache et al. [32] used the Coulomb breakup technique to extract the cross section. Very recently, a direct measurement has been performed at LUNA [1]. The results of this very difficult experiment agree well with those from the indirect method [32]. So, this confirmed low cross section comforts the prediction of the BBN calculations of a low primordial ^6Li value, $^6\text{Li}/\text{H} = 10^{-14}$.

For the remaining of the 391 reactions, we use tabulated μ and σ [35], tabulated limits [3, 17, 24, 81] together with Eqs. (4.6) and (4.7) and for the others, tabulated rates together with estimated uncertainty factors and Eqs. (4.4) and (4.5). In particular, in the work of Coc et al. [17], many rates come from theory (TALYS code) [31] and have not been re-evaluated since then. The TALYS code is obviously not well adapted to this low mass region where level densities are too low to justify the Hauser-Feshbach approach. However, due to the lack

of experimental data it can be used as a first guess for the hundred of reaction rates that are needed. To estimate the uncertainty associated with TALYS rates in the relevant ranges of masses and temperature, Coc et al. [17] compared them with experimentally determined reaction rates [3, 35] and found that the differences do not exceed three orders of magnitude at *BBN temperatures* (see Figs. 1–11 and 16–21 in Coc et al. [17]). In their sensitivity study, they were not found to influence significantly the results, when *individually* multiplied by factors up to $10^{\pm 3}$, except for ten reactions whose rates were re-evaluated. Hence, for the rates, labeled "TALYS" in Table 4 of Coc et al. [17], we use here uncertainty factors of $f=100$ (i.e. $\sigma = \ln(100)$). (Those, labeled "TALYS" in bold face in the same Table were re-evaluated so that calculated uncertainties are available.) For rates provided without calculated uncertainty, labeled e.g. "CF88", "MF89", "Wag69", . . . , (see Refs. in Coc et al. [17]) we generally adopted $f=3$, except when the uncertainty is not provided but is obviously smaller e.g. "Ham10" [32] or "Nag06" where we adopted a 40% uncertainty ($f=1.4$). This may look arbitrary, but one of the main goal of this work is to identify potentially influential reaction rates that may have to be improved in a subsequent stage.

5 Results concerning ${}^4\text{He}$, D, ${}^3\text{He}$ and ${}^7\text{Li}$

Figure 2 displays the ${}^4\text{He}$, D, ${}^3\text{He}$ and ${}^7\text{Li}$ abundances calculated as a function of η by Monte Carlo with the full network, and evaluated rate uncertainties following Coc et al. [17], compared to our previous work with a reduced network [15]. At η_{CMB} , the differences are hardly visible except for ${}^4\text{He}$, due to the updated neutron lifetime. Comparison between columns 2 and 5 in Table 1 shows the evolution of the yields from Coc & Vangioni [15] with the first WMAP results [64] to the recent *Planck* data [55]. The reduced uncertainty on D/H is a direct consequence of the reduced uncertainty on $\Omega_b h^2$ while ${}^7\text{Li}$ uncertainty is still dominated by nuclear uncertainty on the ${}^3\text{He}(\alpha, \gamma){}^7\text{Be}$ rate.

Figure 2 displays the abundances as a function of η and Table 3 those at the *Planck* baryonic density, both for $N_{\text{eff}} = 3$, as defined by Eq. (5.5). When using the last evaluation of Y_p [8] deduced from observations, we obtain $2.19 \leq N_{\text{eff}} \leq 3.63$ at *Planck* baryonic density. This interval is given after corrections to the weak rates [25, 47, 48] have been introduced as discussed in § 3. It includes the correction for non-instantaneous neutrino decoupling in the presence of oscillations, introduced as a constant shift $\Delta Y_p = +0.0002$ [48] instead of a slight increase of $N_{\text{eff}} = 3$ since, if this approximation works for ${}^4\text{He}$, the change for the other nuclides is exactly in the opposite direction of the true one (see Mangano et al. [48] for details). In Figure 2 we also display for visual inspection the results obtained for the limits on effective number of neutrino family $N_{\text{eff}} = 3.30 \pm 0.27$ derived from the CMB only confidence interval [55].

Finally in Table 3, a comparison between this work and the last observational data is proposed; an overall consistency between standard BBN calculation and the observational constraints is presented except for lithium, as explained above: the discrepancy remains of the order of 3.

6 Results concerning ${}^6\text{Li}$, ${}^9\text{Be}$, B, C

Figure 3 displays the ${}^6\text{Li}$, ${}^9\text{Be}$, ${}^{10}\text{B}$, ${}^{11}\text{B}$ and CNO abundances calculated as a function of η including our estimated uncertainties from the Monte Carlo, and a comparison with observations. The displayed uncertainties are obtained by calculating for each value of η , the

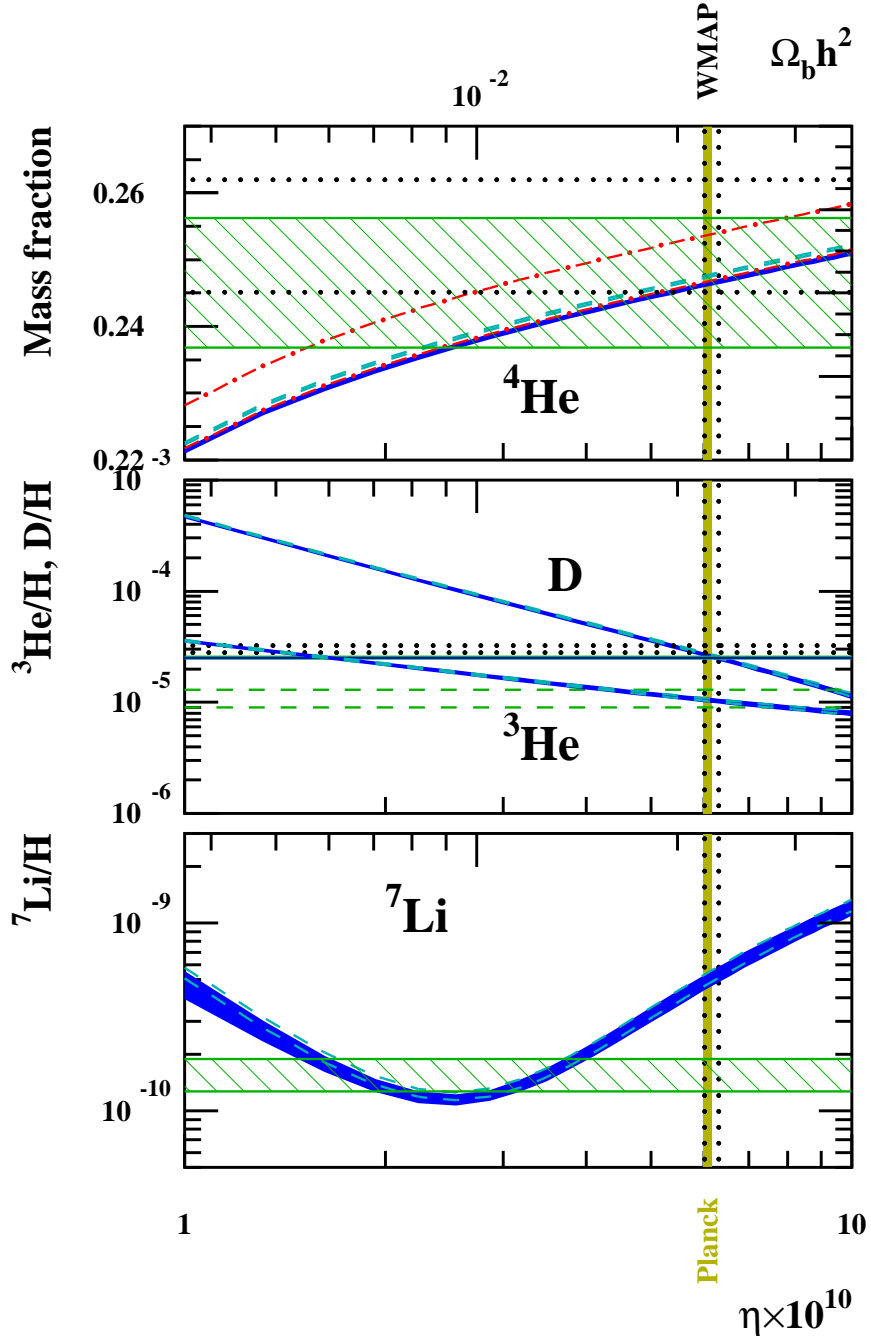


Figure 2. (Color online) ^4He , D, ^3He and ^7Li abundances as a function of η calculated by Monte Carlo with the updated full network (dark blue) or with the reduced network as in Ref. [15] (light blue dashed). The vertical areas correspond i) to the WMAP (dot, black) and ii) *Planck* (solid, yellow) baryonic densities. The horizontal areas (hatched green) represent the adopted observational abundances while the horizontal dotted lines correspond to those previously used [7, 49]. The (red) dash-dotted lines correspond to Y_p calculated with $N_{\text{eff}} = 3.30 \pm 0.27$ derived from the CMB [55].

Table 3. Comparison with observations

	This work	Observations
Y_p^*	0.2461–0.2466	0.2465 ± 0.0097
D/H ($\times 10^{-5}$)	2.57–2.72	2.53 ± 0.04
$^3\text{He}/\text{H}$ ($\times 10^{-5}$)	1.02–1.08	1.1 ± 0.2
$^7\text{Li}/\text{H}$ ($\times 10^{-10}$)	4.56–5.34	$1.58^{+0.35}_{-0.28}$

* See text in § 3.

0.16 and 0.84 quantile [46] of the distributions. The corresponding confidence intervals at η_{CMB} are displayed in Table 4 and are orders of magnitude below observations (§ 2.2).

Table 4. ^6Li to CNO primordial abundances by number.

	Ref. [17]	This work
$^6\text{Li}/\text{H}$ ($\times 10^{-14}$)	1.23	0.90–1.77
$^9\text{Be}/\text{H}$ ($\times 10^{-19}$)	9.60	5.10–26.3
$^{11}\text{B}/\text{H}$ ($\times 10^{-16}$)	3.05	1.85–3.56
CNO/H ($\times 10^{-16}$)	7.43	4.94–28.5

Figure 4 displays the histogram of CNO/H obtained from our Monte Carlo calculation, from which it is possible to extract the 0.16, 0.5 and 0.84 quantile, respectively given by 4.94×10^{-16} , 9.63×10^{-16} and 2.85×10^{-15} . This is very close to the range CNO/H = (0.5 – 3.) $\times 10^{-15}$ estimated by Coc et al. [16] from the results of Coc et al. [17]. However, at high value, the tail of the distribution ($\approx 3\%$) extends to values much above the CNO/H = 10^{-13} limit. At first, it seems straightforward to extract the subset of events, for which e.g. CNO/H > 10^{-13} , and examine the corresponding sampled reaction rates (i.e. the p_k 's in Eq. 4.3) that are stored together with the final abundances in a database. However, since all ≈ 400 p_k 's are different from one realisation to the other, it was not possible to identify combination of reaction rates that produced such an effect. To identify those combinations of reaction rates that allows such high value, we relied upon the calculated correlations between rates and yields.

This method is complementary to the one used by Coc et al. [17], in which a single reaction was tested at a time by changing its rate by factors of 10^n , $n = -3, -2, -1, 1, 2, 3$. Here *all rates are simultaneously changed by factors, different for each reaction*, and randomly sampled as described above. This allows to identify sub-networks rather than individual reactions and takes into account the different uncertainty factors. Results are displayed in Tables 5–12 when their absolute value exceed 10%. ⁴ Note however that a higher sensitivity, as calculated in Coc & Vangioni [15], Coc et al. [17], does not necessarily correspond to a higher correlation as calculated here. Our previous sensitivity studies assumed an arbitrary $\pm 15\%$ rate variation [15] or a factor of up to 1000 rate variation [17]. Here, while, when sampling the rates, we still allow for large arbitrary rate variations for reactions with no

⁴ We use this simple criterion but are aware that more sophisticated criteria need to be developed: see e.g. Fig. 6 in Iliadis et al. [36].

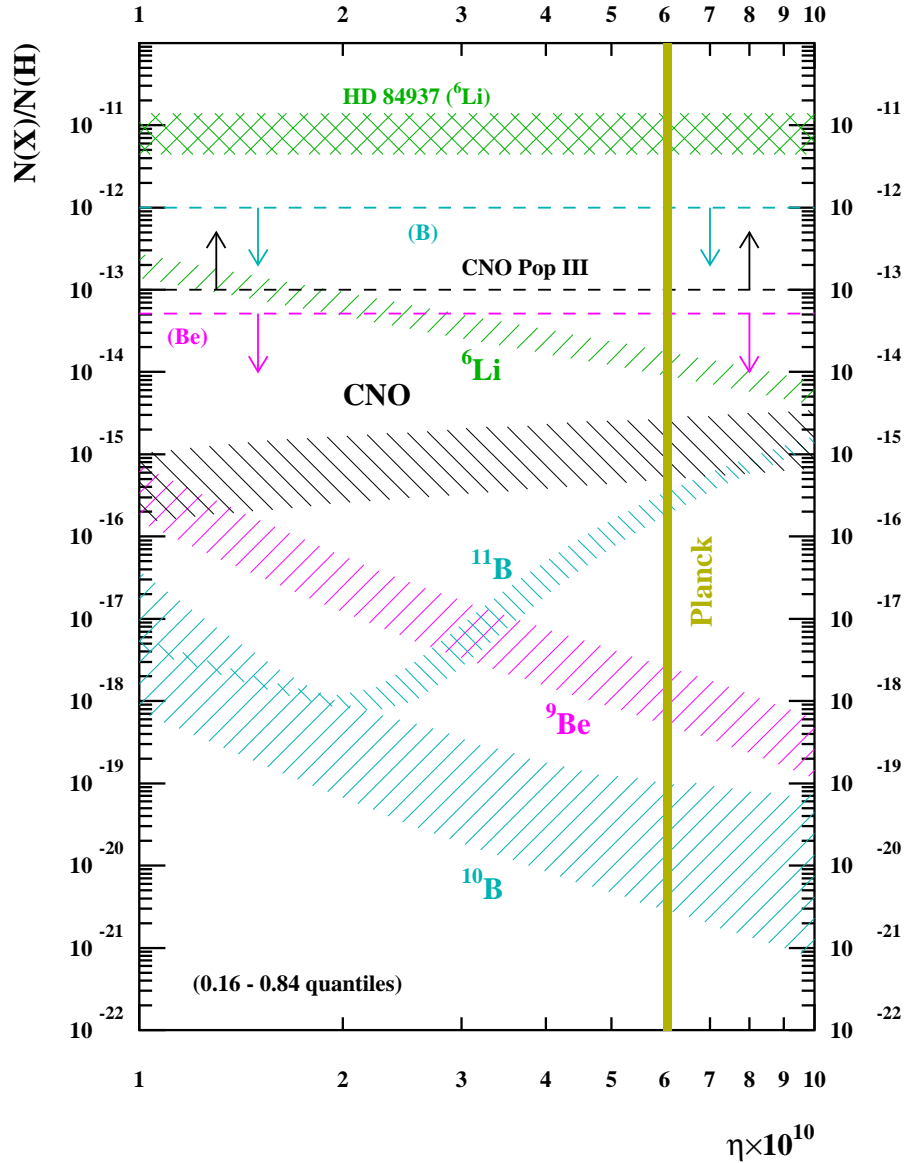


Figure 3. Standard big bang Nucleosynthesis predictions for the abundances of ${}^6\text{Li}$, Be, B and CNO isotopes as a function of baryonic density, compared to some observations. The horizontal lines and areas correspond to the ${}^6\text{Li}$ observation in HD 84937 (green), beryllium (magenta) and boron (light blue) upper limits, and CNO lower limit to affect Population III stars; see text.

documented rate uncertainties, we restrict the variations to evaluated rates and associated uncertainties when available. These latter reactions include e.g. those evaluated by Descouvemont et al. [24] or those identified as influential in a first step, but evaluated in a second step by Coc et al. [17]. For instance, the most influential rate on ${}^7\text{Li}+{}^7\text{Be}$ is ${}^1\text{H}(n,\gamma){}^2\text{H}$ [15] but its rate uncertainty is very small [2] so that it does not appear in the table, contrary to the next most influential, ${}^3\text{He}(\alpha,\gamma){}^7\text{Be}$ whose rate uncertainty is still not negligible and thus

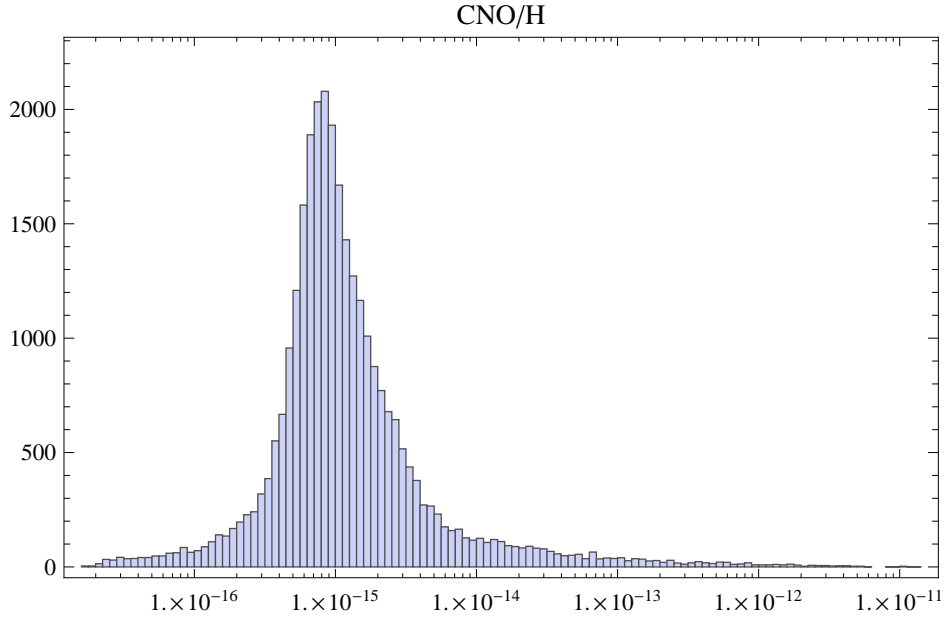


Figure 4. CNO/H distribution showing that high values are obtained in a non negligible proportion.

appears in Table 8.

The reactions that appear most correlated with the isotopes lighter than C (Tables 5–11) are among those found in previous studies. In Table 12, it appears that besides the already known influential reactions on CNO production [17] [${}^7\text{Li}(d,n){}^4\text{He}$, ${}^{12}\text{B}(p,\alpha){}^9\text{Be}$, ${}^8\text{Li}(\alpha,n){}^{11}\text{B}$, ${}^{13}\text{C}(d,\alpha){}^{11}\text{B}$], new influential reactions are found. It indicates a new possible path for CNO production involving ${}^{10}\text{Be}$, namely: ${}^{10}\text{Be}(p,\alpha){}^7\text{Li}$, ${}^{10}\text{Be}(\alpha,n){}^{13}\text{C}$, ${}^7\text{Li}(t,\gamma){}^{10}\text{Be}$, ${}^8\text{Li}(t,n){}^{10}\text{Be}$, ${}^{10}\text{Be}(t,n){}^{12}\text{B}$ and ${}^{10}\text{Be}(p,t){}^4\text{He}$. Note that all these new reactions involve radioactive isotope(s) [${}^3\text{H}$, ${}^8\text{Li}$ and ${}^{10}\text{Be}$] in the initial state, hence the absence of direct experimental data. From this analysis, it is obvious that a new chain of reactions leading to CNO via ${}^{10}\text{Be}$ need further attention as it could, depending on the cross-sections, provide a more efficient source of CNO.

Table 5. Correlations with ${}^4\text{He}$

Reaction	$C_{\text{He4},k}$
$1/\tau_n$	-0.9677
${}^3\text{He}(t, np){}^4\text{He}$	0.1151
$\text{D}(d, n){}^3\text{He}$	0.1282
$\text{D}(d, p){}^3\text{H}$	0.1296

Table 6. Correlations with D

Reaction	$C_{\text{D},k}$
$\text{D}(p, \gamma){}^3\text{He}$	-0.7790
$\text{D}(d, n){}^3\text{He}$	-0.4656
$\text{D}(d, p){}^3\text{H}$	-0.4082

Table 7. Correlations with ${}^3\text{He}$

Reaction	$C_{\text{He3},k}$
$\text{D}(p, \gamma){}^3\text{He}$	0.6699
$\text{D}(d, n){}^3\text{He}$	0.1640
$\text{D}(d, p){}^3\text{H}$	-0.1897
${}^3\text{He}(d, p){}^4\text{He}$	-0.6841

Table 8. Correlations with ${}^7\text{Li}$

Reaction	$C_{\text{Li7},k}$
${}^7\text{Be}(n, \alpha){}^4\text{He}$	-0.3057
${}^7\text{Be}(d, p){}^2{}^4\text{He}$	-0.2079
$\text{D}(p, \gamma){}^3\text{He}$	0.4043
$\text{D}(d, n){}^3\text{He}$	0.1547
${}^3\text{He}(d, p){}^4\text{He}$	-0.2232
${}^3\text{He}(\alpha, \gamma){}^7\text{Be}$	0.7107

Table 9. Correlations with ${}^6\text{Li}$

Reaction	$C_{\text{Li6},k}$
$\text{D}(\alpha, \gamma){}^6\text{Li}$	0.9835
${}^6\text{Li}(p, \alpha){}^3\text{He}$	-0.1333

Table 10. Correlations with ${}^9\text{Be}$

Reaction	$C_{\text{Be9},k}$
${}^7\text{Li}({}^3\text{He}, p){}^9\text{Be}$	0.2820
${}^7\text{Li}(t, n){}^9\text{Be}$	0.8910

Table 11. Correlations with ${}^{11}\text{B}$

Reaction	$C_{\text{B11},k}$
${}^{11}\text{B}+{}^{11}\text{C}$	
$\text{D}(p, \gamma){}^3\text{He}$	0.1081
${}^3\text{He}(\alpha, \gamma){}^7\text{Be}$	0.1621
${}^7\text{Be}(\alpha, \gamma){}^{11}\text{C}$	0.2188
${}^{11}\text{C}(n, \alpha){}^2{}^4\text{He}$	-0.9069

Table 12. Correlations with CNO

Reaction	$C_{\text{CNO},k}$
CNO	
${}^{12}\text{B}(p, \alpha){}^9\text{Be}$	-0.1030
${}^{10}\text{Be}(p, \alpha){}^7\text{Li}$	-0.2479
${}^{10}\text{Be}(\alpha, n){}^{13}\text{C}$	0.2175
${}^7\text{Li}(t, \gamma){}^{10}\text{Be}$	0.1363
${}^8\text{Li}(\alpha, n){}^{11}\text{B}$	0.1449
${}^8\text{Li}(t, n){}^{10}\text{Be}$	0.1958
${}^{10}\text{Be}(t, n){}^{12}\text{B}$	0.1139
${}^{13}\text{C}(d, \alpha){}^{11}\text{B}$	-0.2378
${}^{10}\text{Be}(p, t){}^2{}^4\text{He}$	-0.1297
${}^7\text{Li}(d, n){}^2{}^4\text{He}$	-0.1806

These reactions were not identified in our previous work [17], because we varied the rates, *one at a time*, (by factors of 10^n with n varying from -3 to 3 by steps of one unit). For instance, when increasing the ${}^8\text{Li}(t,n){}^{10}\text{Be}$ or ${}^{10}\text{Be}(\alpha,n){}^{13}\text{C}$ rates by a factor of 1000, the CNO abundance only increase by 30% [17] while if *both* rates are increased by the same factor, CNO/H is found to be higher by a factor of 200. This is the purpose of the following analysis to identify such potential new paths. Hence, we first allowed *all rates to vary simultaneously and independently* according to lognormal distributions. Now, to better identify the chains of reactions that may lead to an increased CNO production, we allow the rates of the 6 newly identified reactions listed above to vary within a few orders of magnitude as in Ref. [17] but considering *all* possible combinations. We chose factors of $10^{\pm 2}$ variations on rates w.r.t. TALYS calculated rates which are consistent with our comparison between TALYS and experimentally measured rates [17] and select those combinations of factors that leads to a CNO/H production higher than 10^{-13} , the minimum value to affect Pop III stars [27]. In Table 13 are displayed the 9 combinations (out of $3^6 = 729$ combinations) of signs in the exponent of the $10^{\pm 2}$ factors (with "0" meaning no rate variation) for which $\text{CNO}/\text{H} > 10^{-13}$. (Obviously, we could have reduced the number of combinations: taking higher/lower rates for production/destruction of ${}^{10}\text{Be}$ but we found it was not worth the trouble.) Table 13, shows that the ${}^7\text{Li}(t,\gamma){}^{10}\text{Be}$ and ${}^{10}\text{Be}(t,n){}^{12}\text{B}$ reactions are not essential since whatever the exponent (-2 , 0 or $+2$) of the variation factor, the result is not significantly affected. On the contrary, the combination of higher rates for ${}^{10}\text{Be}(\alpha,n){}^{13}\text{C}$ and ${}^8\text{Li}(t,n){}^{10}\text{Be}$ together with lower rates for ${}^{10}\text{Be}(p,\alpha){}^7\text{Li}$ and ${}^{10}\text{Be}(p,t){}^4\text{He}$ result in a substantial increase in primordial CNO production. From this combinatorial analysis we could, hence, separate within the set of 6 reaction rates that were weakly correlated to CNO/H those 4 that really matter. The factors of $10^{\pm 2}$ variation w.r.t. TALYS rates is conservative (see § 4.2) so that even higher CNO yields can be expected. Experimental investigations of these four reactions (Fig. 5) are hence highly recommended.

Afterwards, the production of this short list of reactions involving ${}^{10}\text{Be}$ for the production of CNO may seem straightforward but dealing with a relatively large and dense network (i.e. including p, n, α , d, t and ${}^3\text{He}$ induced reactions) is not so easy. First, among all the reaction paths that could connect $A < 8$ to CNO nuclei, the study of correlations allowed us first to identify, the six reactions of Table 13 that did not show up in our (or any other) simpler sensitivity analysis [17] of the same network. Second, the extensive combinatorial analysis allowed us to finally select out four reactions.

Table 13. Each column correspond to a combination of multiplicative factors ("-" for 10^{-2} , "0" for 10^0 and "+" for 10^{+2}) which applied simultaneously to all the six TALYS reaction rates lead to $\text{CNO}/\text{H} > 10^{-13}$.

Reaction	CNO/H > 10^{-13}								
${}^{10}\text{Be}(p,\alpha){}^7\text{Li}$	-	-	-	-	-	-	-	-	-
${}^{10}\text{Be}(\alpha,n){}^{13}\text{C}$	+	+	+	+	+	+	+	+	+
${}^7\text{Li}(t,\gamma){}^{10}\text{Be}$	-	-	-	0	0	0	+	+	+
${}^8\text{Li}(t,n){}^{10}\text{Be}$	+	+	+	+	+	+	+	+	+
${}^{10}\text{Be}(t,n){}^{12}\text{B}$	-	0	+	-	0	+	-	0	+
${}^{10}\text{Be}(p,t){}^4\text{He}$	-	-	-	-	-	-	-	-	-

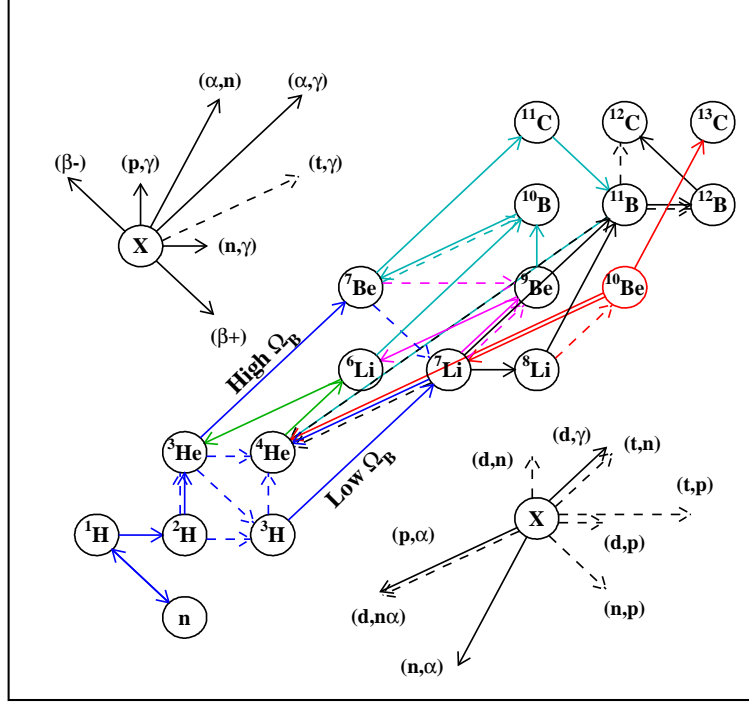


Figure 5. (Color online) BBN nuclear network with in red the new possible paths to CNO.

This work has updated the BBN predictions in order to take into account the most recent developments concerning the cosmological framework (i.e. the cosmological parameters determined from the recent CMB *Planck* experiment). It demonstrates that these predictions are robust for the lightest elements. It shows also that the modification of these parameters in the range allowed cannot alleviate the lithium problem; concerning primordial CNO production we show that higher CNO yields can be expected: the four reaction rates $^{10}\text{Be}(\alpha,n)^{13}\text{C}$, $^8\text{Li}(t,n)^{10}\text{Be}$, $^{10}\text{Be}(p,\alpha)^7\text{Li}$ and $^{10}\text{Be}(p,t)^{24}\text{He}$, could be investigated to test this result.

Finally, we want to emphasize the use of statistical methods in BBN have lead to the identification of a possible new path to CNO. For this, we have used the simple Pearson's correlation coefficient to discriminate important reactions. This is obviously a first step: more elaborate statistical techniques could be developed and also applied to other nucleosynthesis sites [36].

Acknowledgments

This work made in the ILP LABEX (under reference ANR-10-LABX-63) was supported by French state funds managed by the ANR within the Investissements d'Avenir programme

under reference ANR-11-IDEX-0004-02 and by the ANR VACOUL, ANR-10-BLAN-0510. We are indebted to Christian Iliadis and Richard Longland for many fruitful discussions, and in particular on statistical issues concerning reaction rates and nucleosynthesis. We thank warmly the referee for his remarks and very useful comments.

A Appendix: Relation between η and $\Omega_b h^2$

Here, for precise comparison with other works that quote η numerical values rather than $\Omega_b h^2$ ones, we recall here the numerical relationship between the two. This was calculated previously by Steigman [69]; here we detail our own calculation.

What is important for BBN is the baryonic density $\Omega_b \cdot \rho_{0,C}$ where $\rho_{0,C}$ is the present day critical density given by (numerical values of physical constants are taken from Beringer et al. [58], atomic masses from Wang et al. [78]):

$$\rho_{0,C} = \frac{3H_0^2}{8\pi G} = 1.87847 \times 10^{-29} h^2 \text{ g/cm}^3, \quad (\text{A.1})$$

that allows for the calculation of

$$\rho_b(t) = [1.87847 \times 10^{-29} \text{ g/cm}^3] \times \Omega_b h^2 a^{-3}(t), \quad (\text{A.2})$$

to be used in the network calculations. The photon density (number/cm³; $T_0 = 2.7255$ K; $\zeta(3) = 1.20206$) is:

$$n_\gamma(T) = \frac{2\zeta(3)}{\pi^2} \left(\frac{k_B T}{\hbar c} \right)^3 = 410.73 \left(\frac{T}{T_0} \right)^3 \text{ cm}^{-3} \quad (\text{A.3})$$

The number of baryon per photon is thus given by:

$$\eta = \frac{\rho_{0,b}}{n_\gamma(T_0)\bar{M}} \equiv \frac{3H_0^2}{8\pi G} \frac{\pi^2}{\zeta(3)} \left(\frac{\hbar c}{k_B T_0} \right)^3 \left(M_p(1 - Y_p) + \frac{M_\alpha}{4} Y_p \right)^{-1} \Omega_b \quad (\text{A.4})$$

where \bar{M} is the mean baryon mass

$$\bar{M} = M_p(1 - Y_p) + \frac{M_\alpha}{4} Y_p = (1.6735 - 0.0119 Y_p) \times 10^{-24} \text{ (g)}. \quad (\text{A.5})$$

So that the relation between η and $\Omega_b h^2$ are:

$$\eta = 2.7381 \times 10^{-8} \Omega_b h^2 \text{ or } \Omega_b h^2 = 3.6521 \times 10^7 \eta \quad (\text{A.6})$$

for $Y_p=0.27$ (solar, $\bar{M} = 1.6703 \times 10^{-24}$ g) or

$$\eta = 2.7377 \times 10^{-8} \Omega_b h^2 \text{ or } \Omega_b h^2 = 3.6528 \times 10^7 \eta \quad (\text{A.7})$$

for $Y_p=0.246$ (BBN, $\bar{M} = 1.6706 \times 10^{-24}$ g). When using the same values for T_0 (2.725 instead of 2.7255 K here) and Y_p (0.27), our result differs by less than 0.004% from the Steigman [69] one. The uncertainty on the present day CMB temperature ($T_0 = 2.7255 \pm 0.0006$ Beringer et al. [58]) induces an uncertainty of less than 0.07% on the calculated coefficient.

References

- [1] M. Anders, D. Trezzi, R. Menegazzo et al., *Phys. Rev. Lett.* **113** (2014) 042501
- [2] S. Ando, R. H. Cyburt, S. W. Hong & C. H. Hyun, *Phys. Rev. C* **74** (2006) 025809
- [3] C. M. Angulo, M. Arnould, M. Rayet, P. Descouvemont, D. Baye et al., *Nucl. Phys.*, A656 (1999) 3-183 and <http://pntpm.ulb.ac.be/nacre.htm>.
- [4] M. Asplund, D.L. Lambert, P.E. Nissen, P.et al., *Astrophys. J.* **644** (2006) 229
- [5] G. Audi, O. Bersillon, J. Blachot & A. H. Wapstra, *Nucl. Phys.* **A729** (2003) 3
- [6] E. Aver, K. A. Olive & E. D. Skillman, *J. Cosmology Astropart. Phys.* **05**, (2010) 003
- [7] E. Aver, K. A. Olive & E. D. Skillman, *J. Cosmology Astropart. Phys.* **04** (2012) 04
- [8] E. Aver, K. A. Olive & E. D. Skillman, *J. Cosmology Astropart. Phys.* **11** (2013) 17
- [9] T. Bania R. Rood & D. Balser, *Nature* **415** (2002) 54
- [10] A. Boesgaard et al., *Astrophys. J.* **743** (2011) 140
- [11] S. Cassisi & V. Castellani, *Astrophys. J. S.* **88** (1993) 509
- [12] R. Cayrel, M. Steffen et al., *Astron. Astrophys.* **473** (2007) L37
- [13] C. Charbonnel et al., *IAU Symposium 268, "Light Elements in the Universe"*, Cambridge University Press **268** (2010)
- [14] A. Coc, N. Nunes, K. Olive, J.P. Uzan and E. Vangioni *Phys. Rev.* **D76** (2007) 023511
- [15] A. Coc & E. Vangioni, *J. of Physics Conference Series* **202** (2010) 012001
- [16] A. Coc, S. Goriely, M. Saimpert, E. Vangioni & Y. Xu, *American Institute of Physics Conference Series* **1484** (2012) 354
- [17] A. Coc, S. Goriely, Y. Xu, M. Saimpert & E. Vangioni, *Astrophys. J.* **744**, (2012)158
- [18] A. Coc, P. Descouvemont, K. Olive, J.-Ph. Uzan and E. Vangioni *Phys. Rev.* **D86** (2012) 043529
- [19] A. Coc, Proceedings of the 11th International Conference on Nucleus-Nucleus Collisions (NN2012), San Antonio, Texas, USA, May 27 to June 1, 2012, *J. Phys.: Conf. Ser.* **420** (2013) 012136
- [20] A. Coc, J.-P. Uzan & E. Vangioni, *Phys. Rev. D* **87** (2013) 123530
- [21] R. Cooke, M. Pettini, R. A. Jorgenson, M. T. Murphy & C. C. Steidel, *Astrophys. J.* **781** (2014) 31
- [22] R. H. Cyburt & B. Davids, *Phys. Rev. C* **78** (2008) 064614
- [23] R. H. Cyburt, J. Ellis, B. B. Fields et al., *J. Cosmology Astropart. Phys.* **05**, (2013) 14
- [24] P. Descouvemont, A. Adahchour, C. Angulo, A. Coc & E. Vangioni-Flam, *Atomic Data and Nuclear Data Tables* **88**, (2004) 203
- [25] D. Dicus, E. Kolb, A. Gleeson, E. Sudarshan, V. Teplitz & M. Turner, *Phys. Rev. D* **26** (1982) 2694
- [26] D. Duncan et al., *Astrophys. J.* **488** (1997) 338
- [27] S. Ekström, G. Meynet, C. Chiappini, R. Hirschi & A. Maeder, *Astron. Astrophys.* **bf 489** (2008) 685
- [28] B. D. Fields, *ARNPS* **6** (2011) 47
- [29] A. Frebel & J. E. Norris, *published in 'Planets, stars and stellar systems', Springer, Edts T. Oswalt & G. Gilmore* **vol. 5** (2013) p. 55

- [30] R. J. Garcia-Lopez et al., *Astrophys. J. Lett.* **500** (1998) 241
- [31] S. Goriely, S. Hilaire, A. J. Koning, *Astron. Astrophys.* **487** (2008) 767
- [32] F. Hammache et al., *Phys. Rev. C* **82** (2010) 5803
- [33] G. Hinshaw, D. Larson, E. Komatsu, E. et al., *Astrophys. J. S.* **208** (2013)19
- [34] J. C. Howk, N. Lehner, B. D. Fields & G. J. Mathews, *Nature* **489** (2012) 121
- [35] C. Iliadis, R. Longland, A. E. Champagne, J. R. Newton, C. Ugalde, A. Coc & R. Fitzgerald, *Nucl. Phys.*, **A841** (2010) 31
- [36] C. Iliadis, R. Longland, A. Coc, F.X. Timmes & A. E. Champagne, (arXiv:1409.5541 [nucl-ex]), accepted for publication in J. Phys. G Focus issue "Enhancing the interaction between nuclear experiment and theory through information and statistics"
- [37] F. Iocco, G. Mangano, G. Miele, O. Pisanti & P. D. Serpico, *Phys. Rev. D* **75** (2007) 30141
- [38] F. Iocco, G. Mangano, G. Miele, O. Pisanti & P.D. Serpico, *Phys. Rep.* **472** (2009) 1
- [39] F. Iocco, P. Bonifacio & E. Vangioni, *Proceedings of the workshop Lithium in the cosmos, Mem.S.A.It. Suppl.* **22** (2012) 3
- [40] Y. I. Izotov, T. X. Thuan & G. Stasinska, *Astrophys. J.* **662** (2007) 15
- [41] Y. I. Izotov & T. X. Thuan, *Astrophys. J. Lett.* **710** (2010) L67
- [42] Y. I. Izotov, G. Stasińska and N.G. Guseva, *Astron. Astrophys.* **558** (2013) A57
- [43] E. Komatsu et al., *Astrophys. J. S.* **192**, (2011) 18
- [44] D.S. Leonard, H.J. Karwowski, C.R. Brune, B.M. Fisher and E.J. Ludwig, *Phys. Rev. C* **73** (2006) 045801
- [45] K. Lind, J. Melendez, M. Asplund et al., *Astron. Astrophys.* **554** (2013) 96
- [46] R. Longland, C. Iliadis, A. E. Champagne et al., *Nucl. Phys. A* **841** (2010) 1
- [47] R. E. Lopez & M. S. Turner, *Phys. Rev. D* **59** (1999) 103502
- [48] G. Mangano et al, *Nucl. Phys. B* **729** (2005) 221
- [49] K. A. Olive, P. Petitjean, E. Vangioni & and J. Silk, *Mon. Not. R. Astron. Soc.* **426** (2012) 1427
- [50] A. Parikh, J. José, F. Moreno, & C. Iliadis, *Astrophys. J. S.* **178** (2008) 110
- [51] P. Peter & J.-P. Uzan, *Primordial Cosmology* (Oxford University Press) (2009)
- [52] M. Pettini, B. J. Zych, M. Murphy, A. Lewis & C. C. Steidel *Mon. Not. R. Astron. Soc.* **391** (2008) 1499
- [53] M. Pettini & M. Cooke, *Mon. Not. R. Astron. Soc.* **425** (2012) 2477
- [54] R.G. Pizzone, R. Sparta, C.A. Bertulani, C. Spitaleri, M. La Cognata, J. Lalmansingh, L. Lamia, A. Mukhamedzhanov & A. Tumino *Astrophys. J.* **786** (2014) 112 (arXiv:1403.4909 [nucl-ex])
- [55] *Planck* Collaboration XVI, P. A. R. Ade, N. Aghanim et al., arXiv:1303.5076 (2013)
- [56] *Planck* Collaboration XVII, P. A. R. Ade, N. Aghanim et al., Xiv:1303.5077 (2013)
- [57] The Review of Particle Physics, C. Amsler et al., (Particle Data Group) *Phys. Lett. B* **667** (2008) 1
- [58] The Review of Particle Physics, J. Beringer et al., (Particle Data Group) *Phys. Rev. D* **86** (2012) 010001
- [59] E. Rollinde, E.Vangioni & K. A. Olive, *Astrophys. J.* **627** (2005) 666

- [60] S. G. Ryan, T. C. Beers, K. A. Olive, B. D. Fields & J. E. Norris, *Astrophys. J.* **530** (2000) L57
- [61] A. L. Sallaska, C. Iliadis, A. E. Champagne et al., *arXiv:1304.7811* (2013)
- [62] L. Sbordone et al., *Astron. Astrophys.* **522** (2010) 26
- [63] A. Serebrov, V. Varlamov & A. Kharitonov et al., *Phys. Lett. B* **605** (2005) 72
- [64] D. N. Spergel et al., *Astrophys. J. S.* **170** (2007) 377
- [65] D.N. Spergel, R. Flauger & R. Hložek, ([arXiv:1312.3313v1\[astro-ph.CO\]](https://arxiv.org/abs/1312.3313v1))
- [66] F. Spite & M. Spite, *Astron. Astrophys.* **115** (1982) 357
- [67] F. Spite & M. Spite, Proceedings IAU Symposium No. 268, *Light Elements in the Universe 9-13 November, Geneva, Switzerland*, Eds. C. Charbonnel, M. Tosi, F. Primas & C. Chiappini, Cambridge University Press (2010) p. 201
- [68] M. Steffen, R. Cayrel, E. Caffau et al., *Mem. Soc. Astron. It. Suppl.* **22** (2012) 152
- [69] G. Steigman, *JCAP* **10** (2006) 016
- [70] G. Steigman, *Annu. Rev. Nucl. Part. Sci.* **57** (2007) 463
- [71] G. Steigman, *Advances in High Energy Physics* **2012** (2012) 268321
- [72] E. Vangioni-Flam, M. Cassé, B. D. Fields & K. A. Olive, *Astrophys. J.* **468** (1996) 199
- [73] E. Vangioni-Flam, R. Ramaty, K. A. Olive & M. Cassé, *Astron. Astrophys.* **337** (1998) 714
- [74] E. Vangioni-Flam, M. Cassé & J. Audouze, *Physics Reports* **333** (2000) 365
- [75] E. Vangioni-Flam & M. Cassé, *New Astr. Rev.* **45** (2001) 583
- [76] E. Vangioni-Flam et al., *Astrophys. J.* **585** (2003) 611
- [77] B. Wang, C. A. Bertulani and A. B. Balantekin, *Phys. Rev. C* **83** (2011) 018801
- [78] M. Wang, G. Audi, A.H. Wapstra, F.G. Kondev, M. MacCormick, X. Xu, and B. Pfeiffer, *Chinese Physics C* **36** (2012) 1603
- [79] R. V. Wagoner, *Astrophys. J. S.* **162** (1969) 247.
- [80] F. Wietfeldt & G. Greene, *Rev. Mod. Phys.* **83** (2011) 1173
- [81] Y. Xu, K. Takahashi, S. Goriely, M. Arnould, M. Ohta & H. Utsunomiya, *Nucl. Phys. A* **918** (2013) 61